

DOI: 10.1002/cbic.200700608

## Rapid Identification of a Protein Binding Partner for the Marine Natural Product Kahalalide F by Using Reverse Chemical Proteomics

Andrew M. Piggott and Peter Karuso\*<sup>[a]</sup>*Dedicated to the memory of Professor Paul J. Scheuer*

Kahalalide F (KF) is in phase II clinical trials as an anticancer drug against a range of difficult to treat solid tumors including prostate, breast and colon carcinomas, neuroblastomas, chondrosarcomas, and osteosarcomas and has relatively low toxicity to nontumor cells.<sup>[1]</sup> KF was originally isolated by Hamann and Scheuer from the sacoglossan marine mollusk, *Elysia rufescens*, and subsequently from the sacoglossan's food source, the green alga *Bryopsis* sp.<sup>[2,3]</sup> In phase I clinical trials, KF had a clinical benefit for patients with advanced androgen refractory prostate cancer and other advanced tumors.<sup>[4]</sup> KF appears to act on cell lysosomes, with treated cells swelling dramatically and forming large vacuoles. Cell death is thought to occur via oncosis,<sup>[5]</sup> with KF inducing sub G1 cell-cycle arrest and cytotoxicity independently of MDR, HER2, p53, and bcl-2.<sup>[6]</sup> A recent study by Janmaat et al.<sup>[7]</sup> showed that sensitivity to KF in a variety of cell lines was positively correlated to receptor protein tyrosine kinase ErbB3 (HER3) levels and that KF efficiently inhibited the phosphatidylinositol 3-kinase-Akt signaling pathway in sensitive cell lines. These findings suggest that KF is involved in a hitherto unknown oncosis signaling pathway and that disruption of lysosomes is simply the final step in a series of cascading events. Despite numerous studies into the mode of action of KF, the actual cellular receptor for the molecule remains a mystery.

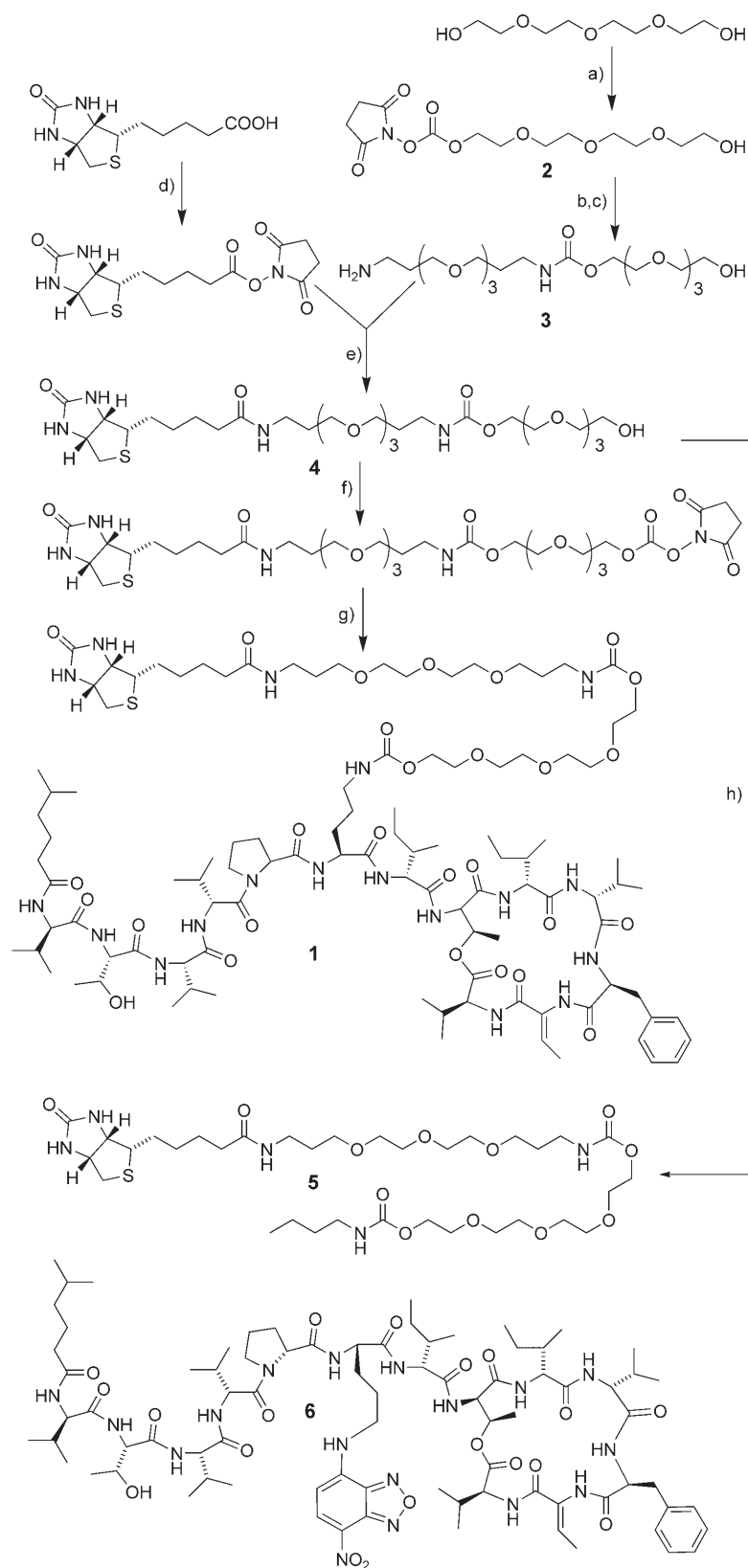
Chemical proteomics<sup>[8]</sup> is a powerful tool for isolating and identifying cellular receptors for biologically active natural products, thereby facilitating subsequent rational drug design, and often providing valuable information regarding underlying biochemical and cellular processes. In chemical proteomics, a small molecule (drug) is immobilized on a solid support or is tagged with a radioactive/fluorescent label to generate an activity or affinity probe, which can be used to isolate and identify a single protein or a family of proteins from an entire proteome.<sup>[9]</sup> However, this technique often requires larger amounts of protein than are typically available in such experiments, particularly for low-abundance proteins, and more importantly, generally results in isolation of the most abundant binding protein, rather than the most avid binder.<sup>[10]</sup> One solution is to provide a physical link between the protein and its corresponding gene—the so-called “genotype–phenotype link”.<sup>[11]</sup> This construct allows affinity purification of the protein

using an immobilized natural product, but also provides a means of identification through amplification (PCR) and sequencing of the attached gene. Whereas there are several methods of creating a genotype–phenotype link, such as mRNA display<sup>[12]</sup> and ribosome display,<sup>[13]</sup> currently the most popular is phage display,<sup>[14]</sup> whereby the gene encoding a protein of interest is cloned into a bacteriophage (phage) in such a way that the protein is expressed on the surface of the virus. If an entire cDNA library is cloned into a phage display vector, each phage particle will contain a different gene insert and will express the protein encoded by that gene on its surface. The displayed proteins usually behave as if they were free in solution and do not suffer from many of the problems associated with protein overexpression in bacterial cells, such as toxicity or precipitation. Phage displaying the target protein can then be isolated from the library using an immobilized natural product, as per standard chemical proteomics experiments.<sup>[15,16]</sup> The real power of phage display comes from the fact that phages can be amplified by transfection into *E. coli* and then subjected to another round of affinity selection with the immobilized small molecule. This cycle can be repeated numerous times, allowing the most avid binder(s) to be identified, even if they are only present in very small amounts in the original cDNA library. As the starting point is actually a transcriptome and not a proteome, we call this technique “reverse chemical proteomics”.<sup>[9]</sup> A potential problem with all chemical proteomics and reverse chemical proteomics methods is that derivatization of the small molecule may affect its biological activity and this possibility must first be excluded. In this paper, we describe the first use of reverse chemical proteomics with T7 phage display to isolate a human protein binding partner for a marine natural product with no known receptor.

A biotinylated analogue of KF **1**, containing a long, hydrophilic linker, was synthesized (Scheme 1) and immobilized on a neutravidin-coated microtiter plate to generate an affinity support. In addition, a biotinylated control reagent, biotin-Bu **5**, was synthesized by coupling **4** with n-butylamine to mimic only the ornithine side chain of KF. KF-NBD **6**, a fluorescent analogue of KF, also derivatized through the primary amine of the ornithine side chain of KF with 4-chloro-7-nitro-2,1,3-benzoxadiazole (NBD) was similarly made for fluorescence microscopy (Figure 1). It has been shown that the biological activity of KF is lost on hydrolysis of the cyclic ester to give kahalalide G,<sup>[3]</sup> suggesting that the hexadepsipeptide ring is required for activity. As the ornithine side chain of KF is some distance from the depsipeptide ring and derivatization of this group has been shown to result in retention of anticancer activity,<sup>[17]</sup> it was reasoned that this group might not be important for

[a] Dr. A. M. Piggott, Prof. P. Karuso  
Department of Chemistry and Biomolecular Sciences, Macquarie University  
Sydney, NSW, 2109 (Australia)  
Fax: (+61) 2-9850-8313  
E-mail: peter.karuso@mq.edu.au

Supporting information for this article is available on the WWW under <http://www.chembiochem.org> or from the author.



**Scheme 1.** Synthesis of biotin-KF 1. Reagents and conditions: A) DSC, Hünig's Base, MeCN, 25 °C, 16 h, not isolated; B) Boc-NH-TEG-NH<sub>2</sub>, Hünig's Base, MeCN, 25 °C, 4 h, 57%; C) TFA (neat), 25 °C, 5 min, quant; D) NHS, DCC, THF/DMSO, 25 °C, 18 h, 71%; E) Et<sub>3</sub>N, MeCN/DMSO, 25 °C, 4 h, 74%; F) DSC, Et<sub>3</sub>N, MeCN, 25 °C, 16 h, 73%; G) kahalalide F, Et<sub>3</sub>N, MeCN/DMSO, 25 °C, 16 h, 85%; H) DSC, TEA, DMSO/acetonitrile 25 °C, 16 h, then *n*-butylamine 4 h, 44%.

binding of KF to its receptor(s). This was supported by microscopy of human cell lines treated with 1 and 6 (Figure 1). In both cases, the KF analogue was able to enter the cells, causing death within minutes at 10  $\mu$ M.

It has previously been reported that KF causes profound vesiculation and eventually bursts cancer cells leaving only the nucleus intact but granulated.<sup>[18]</sup> We observed detachment of confluent cells followed by extensive blebbing and then lysis of the cell membranes (see Figures S9–S11 in the Supporting Information). The nuclear membrane was unaffected by the derivatives and free nuclei were visible shortly after treatment with KF or analogues. Some nuclear granulation was observed by phase contrast microscopy (Figure 1 B) of OVCA429 cells.

Three T7 phage-displayed human disease cDNA libraries (Alzheimer brain, breast tumor, and lung tumor) were subjected to nine rounds of selection using the KF-derivatized plate as an affinity probe. Brief washing was used for the first five rounds of selection to ensure that low affinity binders present in low copy numbers were not lost. This resulted in the accumulation of nonspecific binders and those with a growth advantage (for example, überphage with no insert; 175 bp band in Figure 2C). Consequently, a further four rounds of selection were performed, with more rigorous washing steps between each round, which resulted in the loss of überphage and appearance of new bands (Figure S7). The selection was terminated before consensus to uncover a wider selection of possible receptors. Random plaques were selected from each library and their DNA inserts were amplified by PCR and fingerprinted with *Hinf*I.

Sequencing the DNA insert from every clone isolated to determine its identity is both time consuming and costly. Therefore, we employed the restriction endonuclease *Hinf*I, which is a frequent base cutter commonly used for analysis of genomic DNA,<sup>[19]</sup> to create a DNA fingerprint of each clone. By performing gel electrophoresis on the digested DNA and examining the unique pattern of bands produced (Figure 2), it is possible to identify clones containing identical or similar DNA inserts, thereby reducing the amount of sequencing required. Thus nine clones in the Alzheimer brain library, two clones in the breast tumor library, and four clones in the lung tumor library all had very similar DNA fingerprints. Subsequent DNA sequencing of these clones revealed that all 15 contained a copy of the human ribosomal protein S25 (RPS25) gene that was in frame with the T7 coat protein, with the only difference between clones being in the length of the sequences at the start and end of the gene (Figure S12). Each T7 phage display library contains approximately 10<sup>7</sup> primary clones, so the probability of rescuing two nonidentical clones expressing the same protein from the same library

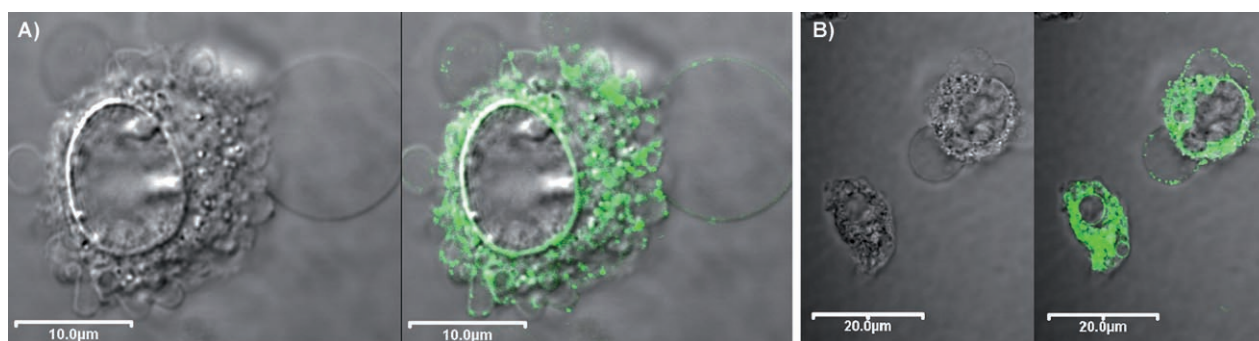


**Figure 1.** Phase contrast and fluorescence microscopy of A) HOSE1.7 and B) OVCA429 cells treated with **6** ( $10\ \mu\text{M}$ ) for 15 min show extensive vesiculation of cytoplasm characterized by blebbing before lysis. The nuclear membranes are unaffected. In both cell lines, the fluorescently labeled KF stained specific structures in the cytoplasm.

by chance is 1 in  $10^7$ , as is the probability of isolating clones expressing the same protein (Figure S8) from two different cDNA libraries. The possibility of contamination from one selection to another can be excluded because each library yielded different clones. Therefore, the concentration of at least five different RPS25 clones from three different cDNA libraries is highly significant and suggests that RPS25 is a binding partner for KF. Apart from RPS25, no other interesting clones were enriched by the KF support. Two clones isolated from the breast tumor library (Supporting Information) contained a fragment of DNA with no assigned function. The peptide encoded by this fragment showed homology with ovarian epithelial carcinoma related protein, which is a putative cancer marker<sup>[20]</sup> but the peptide was out of frame with the coat protein (+1) so is unlikely to be expressed by the phage. Two clones for a hypothetical protein (FLJ20297) were also isolated from the breast tumor library but the small fragment was also out of frame (+1). Similarly, two clones for a small section of chromosome 1 were isolated from the lung tumor library but there is a stop codon very soon after the beginning of the insert in all three reading frames. Thus only RPS25 was isolated from all three libraries as in-frame, full-length clones. No other clone was isolated from multiple libraries and multiple clones from within one library did not contain in-frame proteins of any length. One clone isolated from the lung tumor library was found to display a full-length, out-of-frame (−1) copy of proline rich nuclear receptor co-activator 2. This cDNA sequence also contains several stop codons in the long 5′-UTR so is unlikely to actually express any protein.

An on-phage binding assay<sup>[16]</sup> was used to determine whether the five different T7 phage-displayed RPS25 clones have a greater affinity for neutravidin plates derivatized with **1** than for similar plates derivatized with **5**. It was found that all five RPS25 clones isolated, including those missing the first 11 amino acid residues of the protein (BrTE5/LuTE4), had a higher affinity for a microtiter plate derivatized with **1** than **5** (Figure 3A). In contrast, wild-type phage (überphage) showed a low affinity for both surfaces. To estimate the dissociation constant for the RPS25–KF interaction, a second on-phage binding assay was also performed using free KF to elute bound phage specifically. It was discovered that incubation with solutions of

KF in PBS for 30 min at room temperature resulted in complete elution of bound phage, regardless of KF concentration (Figure S6). Reducing the incubation time to 10 min produced a clear dose-response between KF concentration and phage titer (Figure 3B). Although the phage titer had not reached a maximum at  $100\ \mu\text{M}$  KF, higher concentrations were not attainable because of limited solubility. Therefore, the titers obtained from the 30 min elution were used to estimate the maximum number of elutable phage ( $4.8 \times 10^7$  pfu mL<sup>−1</sup>). The data were fitted to a four parameter logistic equation using least squares regression and the EC<sub>50</sub> value for the RPS25–KF interaction was found to be  $50 \pm 30\ \mu\text{M}$ .

Surface plasmon resonance (SPR) was used to confirm the selectivity of phage-displayed RPS25 for binding to **1** over a control chip. Concentrated RPS25–phage lysate was passed over a streptavidin-coated gold chip that had been derivatized with either **1** or **5** (control), and the association and subsequent dissociation in buffer were monitored by SPR (Figure 3C). In addition, RPS25-phage and überphage (displaying no foreign protein) were injected over a streptavidin-coated gold chip that had been derivatized with **1** to observe differences in binding kinetics (Figure 3D). RPS25-phage bound more efficiently and at a faster initial rate suggesting a specific interaction. However, as significant nonspecific binding of RPS25-phage to the reference channel **5** and überphage to the KF channel **1** were also observed, it was not possible to analyze the kinetics quantitatively.

Human RPS25 forms part of the small (40S) subunit of the eukaryotic ribosome.<sup>[21]</sup> In eukaryotic cells, ribosomal proteins are synthesized in the cytoplasm and are then transported into the nucleus, where they are assembled into functional ribosomes in the nucleolus.<sup>[22]</sup> As no staining of the nucleus was observed on exposure to **6** (Figure 1), but cytoplasmic structures that could be interpreted as ribosomes were specifically stained, it is possible that KF binds tightly only to assembled functional ribosomes. RPS25 is known to lie at the surface of the mammalian 40S ribosomal subunit and is thought to play a role in stabilizing the conformation of the complex.<sup>[23]</sup> Consequently, interactions between KF and the less basic domain of RPS25 from residue 44 onwards may serve to destabilize the 40S subunit, also preventing the formation of functional ribo-

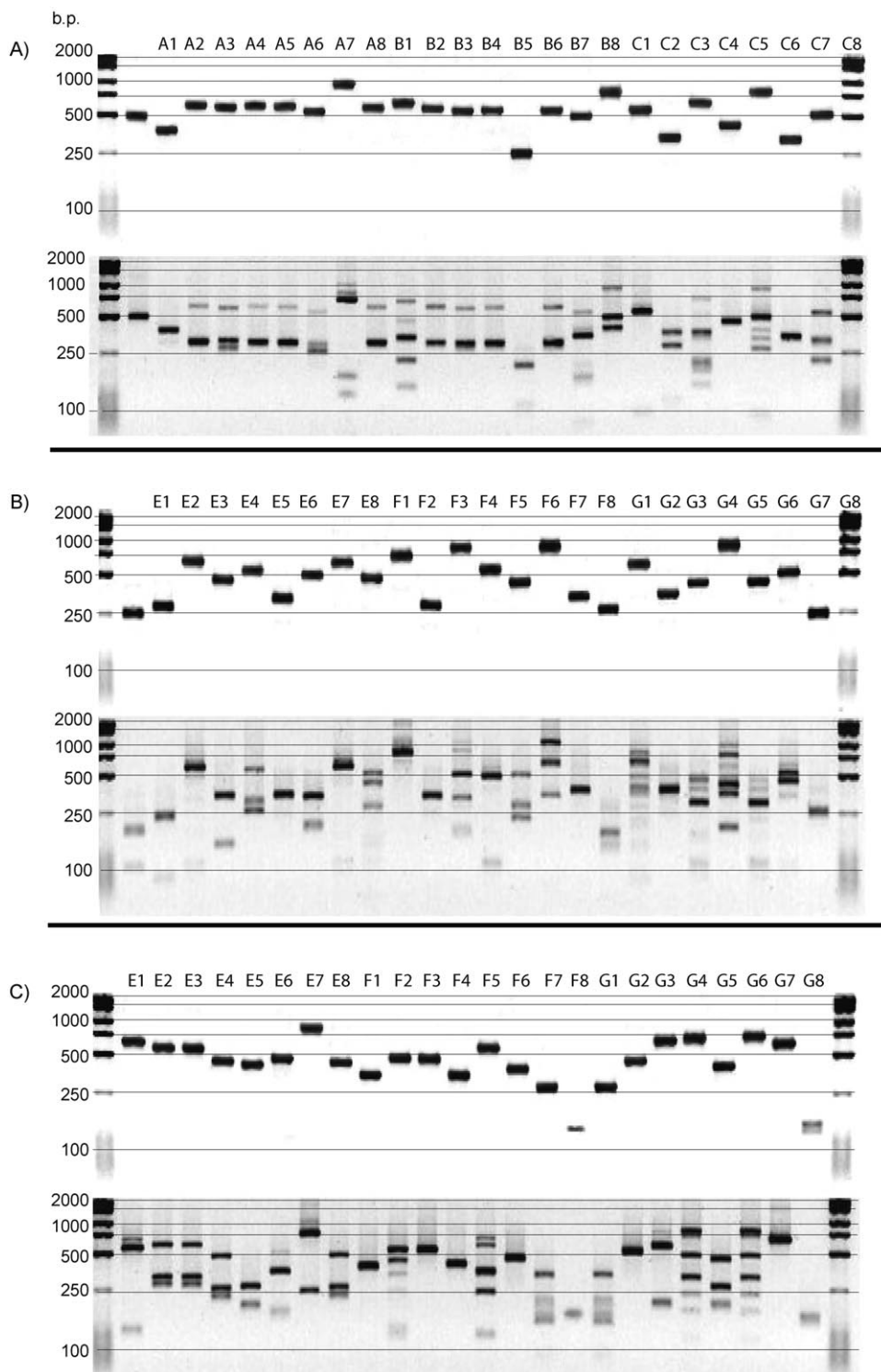


**Figure 2.** Agarose gel electrophoresis of PCR products obtained from individual plaques after nine rounds of selection with **1** immobilized on a neutravidin-coated plate. The DNA inserts were also digested with *Hin*I to produce unique DNA fingerprints of each clone. A) Alzheimer brain (AB), B) Breast tumor (BrT), and C) Lung tumor (LuT) libraries.

somes and inhibiting protein synthesis. However, this mode of action alone is unlikely to result in the rapid swelling and vesiculation of cells observed on treatment with KF.<sup>[18]</sup> It is possible that RPS25 is part of a signaling pathway, and that inter-

action with KF triggers a series of cascading events, eventually resulting in disruption of lysosomal membranes and cell death by oncosis. There have been numerous reports of ribosomal proteins having extraribosomal functions.<sup>[24]</sup> RPS25 is over-expressed in human leukemia (HL60) cells that are resistant to the anticancer drug adriamycin (doxorubicin)<sup>[25]</sup> and is thought to participate in a p53-mediated apoptotic sequence following prolonged starvation of cells.<sup>[26]</sup> In addition, a defect in ribosome biogenesis has been shown to cause activation of a p53-mediated checkpoint, leading to cell cycle block and potential DNA damage.<sup>[27]</sup> Small molecules that bind to ribosomes are known, with the prokaryotic ribosomal subunits being the target of many different classes of antibiotics.<sup>[28]</sup> The majority of these drugs are thought to interact with ribosomal RNA (rRNA) and not with the ribosomal proteins,<sup>[29]</sup> although given that these two components are intimately associated in a functional ribosome, it is possible that both play a role in the binding interactions. Therefore, it would be reasonable to expect that KF would bind much more strongly to an intact ribosome than to isolated RPS25. This phenomenon has been observed with erythromycin, which shows only moderate affinity for ribosomal protein L15 in solution ( $K_d = 20 \mu\text{M}$ ),<sup>[30]</sup> yet binds 2000 times more strongly to the intact 70S ribosome ( $K_d = 10 \text{ nM}$ ).<sup>[31]</sup>

In conclusion, we have used reverse chemical proteomics with T7 cDNA phage display to identify human RPS25 as a binding partner for KF, and have shown that KF binds to phage-displayed RPS25 in a dose-dependent manner with a conservative dissociation constant of  $\sim 50 \mu\text{M}$ . By using an SPR on-phage binding assay we were able to show that RPS25-phage bind specifically to KF, but were unable to determine the rate constants involved because

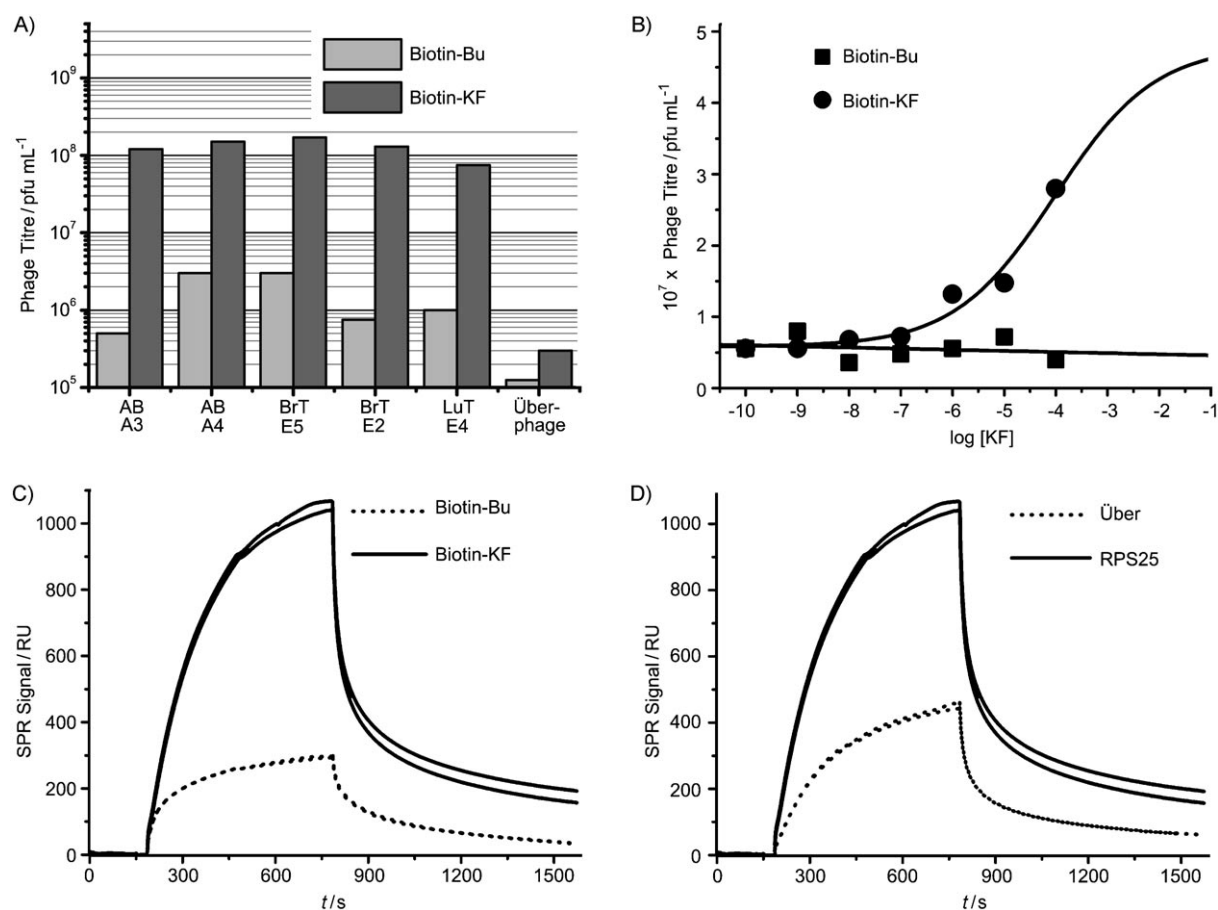


**Figure 3.** On-phage microtiter plate and SPR binding studies. A) Affinity of five T7 phage-displayed RPS25 clones for a neutravidin-coated microtiter plate derivatized with **1**, as determined by nonspecific elution with SDS. B) Affinity of T7 phage-displayed RPS25 plaque ABA3 for a neutravidin-coated microtiter plate derivatized with **1**, as determined by specific elution with KF in PBS. C) SPR sensorgrams for RPS25-phage flowing over streptavidin-coated gold chips derivatized with **1** (solid line) or **5**. D) Comparison of RPS25-phage (solid lines) and wild-type phage (dotted lines) binding to a streptavidin-coated gold chip derivatized with **1**, normalized for concentration.

of high levels of nonspecific binding of the phages or other components of the cell lysate to derivatized surfaces. Currently, the main problems with phage display as a discovery engine appears to be from promiscuous, nonspecific binding and the growth advantage of phage with small inserts. We have overcome the former by preadsorbing the phage library onto a control surface. Whereas more work needs to be done to optimize this technique to minimize background, the data presented herein show that the technique has the potential for the rapid identification of protein binding partners for any small molecule. We hope these results will stimulate other researchers to investigate the significance of the interaction between KF and RPS25 as it is possible that RPS25 is part of a hitherto undiscovered signaling pathway. Future work in our lab includes the incorporation of a photocleavable linker<sup>[32]</sup> to allow specific elution of only bound phages and the derivatization of a range of KF analogues to determine the structural requirements for RPS25 binding. The *HinfI* fingerprinting used in this study allows many clones to be screened very quickly and cheaply, thereby facilitating the analysis of a far greater number of phages without the need for sequencing.

## Experimental Section

**Synthesis of reagents:** Full details of the synthesis and characterization of biotin-KF (**1**), as outlined in Scheme 1, as well as biotin-Bu (**5**), and KF-NBD (**6**) are given in the Supporting Information.

**Microscopy:** Normal human ovarian surface epithelial cells (HOSE1.7) and highly invasive human ovarian carcinoma (OVC A429) cells were obtained from the Australian proteome analysis facility (APAF). Cells were grown in Dulbecco's Modified Eagle Medium (Gibco) and supplemented with HEPES (10 mM), penicillin (1%), glutamine (2 mM), and dialyzed fetal calf serum (20%). Cells were harvested with trypsin/EDTA (Gibco) and grown to ~90% confluency in chambered coverslips (LabTek). For live cell imaging the growth medium was replaced with PBS. Microscopy was performed on an Olympus IX70 inverted confocal microscope (60× oil immersion lens) at the Macquarie university microscopy unit. KF and derivatives were dissolved in DMSO (1 mg mL<sup>-1</sup>) and diluted into PBS before inoculation into confluent cells to obtain a final concentration of 10 µg mL<sup>-1</sup>. Fluorescence excitation was achieved with an argon ion laser (488 nm) with a 510 nm long pass filter.

**Preparation of biotin-KF derivatized microtiter plates:** A solution of biotin-KF (**1**) (1 mg) in DMSO (1 mL) was diluted to 20 mL with

PBS and an aliquot (100  $\mu\text{L}$ ) was added to each well of a neutravidin-coated polystyrene microtiter plate. The plate was left to stand at 4 °C overnight before the solutions were aspirated and each well was washed with PBS (3  $\times$  250 mL). A second plate was derivatized with biotin-Bu (5) in a similar fashion. All microtiter plate wells were preincubated with PBS (250  $\mu\text{L}$ ) for 1 h at room temperature then washed with PBS (3  $\times$  250 mL) immediately before use.

**Affinity selections:** Initial T7 phage libraries and subsequent sublibraries were amplified using *E. coli* BLT5615 as described in the T7 Select system manual.<sup>[33]</sup> Tween-20 (1% in PBS) was added to each clarified T7 phage lysate to give a final concentration of 0.01% and an aliquot of each lysate (100  $\mu\text{L}$ ) was added to the control plate derivatized with biotin-Bu. After incubating for 2 h at room temperature, the lysates were transferred to the plate derivatized with biotin-KF, and left to incubate for 4 h at room temperature. Finally, each well of the plate was washed with phage wash buffer (PWB) (3  $\times$  250 mL over 10 s) and incubated with SDS (1%; 100  $\mu\text{L}$ ) for 30 min at room temperature. The SDS eluates were used to reinfect *E. coli* for the next round of selection, with nine rounds being performed in total. The stringency of the washing step was increased for each successive round, from 3  $\times$  250 mL PWB over 10 s in round 1 to 30  $\times$  250 mL PWB over 5 min in round 9.

**Titering T7:** LB agarose (5 mL) was heated in a microwave oven until completely molten and then allowed to cool to 50 °C. IPTG (24%; 5  $\mu\text{L}$ ) and IPTG-treated BLT5615 cells (250  $\mu\text{L}$ ) were added to the cooled agarose and the mixture was poured onto a prewarmed LB agar plate. The uncovered plate was left to stand at room temperature until the agarose had set completely (30–45 min). The phage eluate retained from each round of selection was serially diluted with 2xYT from 10<sup>-1</sup> to 10<sup>-6</sup> in a flexible 96-well assay plate. A small aliquot (2.5  $\mu\text{L}$ ) of each dilution from each round of selection was dropped onto the surface of the solidified agarose using a multichannel micropipette (8  $\times$  6 array). The uncovered plate was left to stand at room temperature until the drops had absorbed completely into the agarose and was then incubated for 3–4 h at 37 °C until plaques were clearly visible against the lawn of bacteria. The particular phage dilution from each round of selection that contained a countable number of plaques (5–50) was used to calculate the phage titer.

**Picking plaques:** Amplified phage lysate from the final round of selection was serially diluted with 2xYT from 10<sup>-1</sup> to 10<sup>-7</sup> in a flexible 96-well assay plate. A top agarose plate containing an aliquot of the 10<sup>-7</sup> phage dilution (50  $\mu\text{L}$ ) was incubated at 37 °C until plaques were clearly visible against the lawn of bacteria (3–4 h). Individual plaques (96) were collected by stabbing the center of each plaque with a 10  $\mu\text{L}$  micropipette tip and transferring the tip to IPTG-treated BLT5615 cells (100  $\mu\text{L}$  per well) in a 96-well microtiter plate. After 96 plaques had been picked, the microtiter plate was incubated at 37 °C until complete lysis of the bacterial cells in each well was observed (1–2 h). The plate was then centrifuged at 4300 rpm for 10 min at 4 °C, and the supernatant from each well (40  $\mu\text{L}$ ) was transferred into a clean 96-well microtiter plate containing 80% glycerol (10  $\mu\text{L}$  per well) and stored at -80 °C until required.

Of the 96 plaques, 23 small to medium sized plaques were randomly selected for sequencing.

**Hinf1 fingerprinting:** Phage lysate (1  $\mu\text{L}$ ) was added to PCR master mix (49  $\mu\text{L}$ ) and the resulting solution was subjected to 35 rounds of thermocycling using the protocol shown in Table S2. An aliquot of the amplified DNA solution (20  $\mu\text{L}$ ) was then incubated with DNA fingerprinting mix (*Hinf1* 0.1 U, NEB buffer; 30  $\mu\text{L}$ ) at

37 °C for 2 h. Each amplified cDNA insert or fingerprinting sample (5  $\mu\text{L}$ ) was analyzed by gel electrophoresis (1.5% agarose) and visualized by using a UV transilluminator (ethidium bromide).

**Binding assays:** An aliquot of clarified phage lysate (100  $\mu\text{L}$ ) from a single T7 plaque was added to eight wells of a microtiter plate that had been derivatized with the biotin-Bu (5), and a second aliquot (100  $\mu\text{L}$ ) was added to eight wells that had been derivatized with biotin-KF (1). The plates were left to stand for 2 h at room temperature. The lysates were then aspirated and the wells were washed with PWB (10  $\times$  250 mL). For nonspecific elutions, SDS (1%; 100  $\mu\text{L}$ ) was added to each well and the plates were incubated for 30 min at room temperature. For specific elutions, a serial dilution of free KF was performed in PBS and an aliquot of each dilution (100  $\mu\text{L}$ ) was added to one well of the derivatized plate and one well of the control plate and the plates were left to stand for 10 min at room temperature. Finally, the eluates were serially diluted and titered.

**SPR experiments:** SPR experiments were performed on a Biacore 2000 instrument (Biacore AB, Sweden) on streptavidin (SA) chips using a flow rate of 20  $\mu\text{L min}^{-1}$ . Initially, two channels of a Biacore SA SPR chip were conditioned with three consecutive 20  $\mu\text{L}$  injections of 50 mM NaOH in 1 M NaCl and then equilibrated with HBS-EP (10 mM HEPES pH 7.4, 150 mM NaCl, 3 mM EDTA, 0.005% polysorbate 20) for 1 h. A solution of biotin-Bu (5; 10  $\mu\text{M}$ ) in HBS-EP was injected through the first (reference) channel of the chip for 10 min and a solution of biotin-KF (1; 10  $\mu\text{M}$ ) in HBS-EP was similarly injected through the second channel for 10 min. Both channels were then equilibrated with HBS-EP for 1 h.

Clarified RPS25 phage lysate (100  $\mu\text{L}$ ) was filtered (0.22  $\mu\text{m}$ ) and PEG-precipitated according T7Select system manual.<sup>[33]</sup> The phage pellet was resuspended in HBS-EP (1 mL) and the resulting solution was titered and found to be 6.6  $\times$  10<sup>-10</sup> M. Wild-type phage with no insert were grown under identical conditions, precipitated, and resuspended to give a final concentration of 1.3  $\times$  10<sup>-9</sup> M. The biotin-Bu and biotin-KF channels on the SPR chip were injected with phage lysate for 10 min and the association of phages to the chip surface was measured, with one reading taken every second. The channels were then injected with HBS-EP for 15 min and the dissociation of bound phages was recorded in the same manner. Finally, each channel was treated with PWB for 5 min to regenerate the surface of the chip. Each phage solution was injected twice, yielding a total of two association curves and two dissociation curves per phage lysate. The data were then edited manually to remove spikes and baseline anomalies.

## Acknowledgements

The authors would like to thank Edit Pleskonics (Macquarie University) and the Macquarie University Microscopy Unit (Debra Birch) for the confocal microscopy images, Rohit Saldanha (APAF) for supplying the human cell lines, Paul Worden (Macquarie University) for DNA sequencing, and the late Prof. Paul Scheuer (University of Hawaii) for his generous gift of *kahalalide F*.

**Keywords:** bioorganic chemistry · biotinylation · marine natural products · phage display · reverse chemical proteomics

- [1] S. G. Gómez, J. A. Bueren, G. T. Faircloth, J. Jimeno, B. Albella, *Exp. Hematol.* **2003**, *31*, 1104–1111; A. P. Brown, R. L. Morrissey, G. T. Faircloth, B. S. Levine, *Cancer Chemother. Pharmacol.* **2002**, *50*, 333–340.
- [2] M. T. Hamann, P. J. Scheuer, *J. Am. Chem. Soc.* **1993**, *115*, 5825–5826.
- [3] M. T. Hamann, C. S. Otto, P. J. Scheuer, *J. Org. Chem.* **1996**, *61*, 6594–6600.
- [4] J. M. Rademaker-Lakhai, S. Horenblas, W. Meinhardt, E. Stokvis, T. M. de Reijke, J. M. Jimeno, L. Lopez-Lazaro, J. A. Lopez Martin, J. H. Beijnen, J. H. M. Schellens, *Clin. Cancer Res.* **2005**, *11*, 1854–1862; C. Ciruelos, T. Trigo, J. Pardo, L. Paz-Ares, N. Estaun, C. Cuadra, M. Dominguez, A. Marin, J. Jimeno, M. Izquierdo, *Eur. J. Cancer* **2002**, *38*, S33; M. T. Hamann, *Curr. Opin. Mol. Ther.* **2004**, *6*, 657–665; A. Rothe, R. J. Hosse, B. E. Power, *FASEB J.* **2006**, *20*, 1599–1610, 1510 1096/fj 1505–5650rev; G. Hummel, U. Reineke, U. Reimer, *Mol. Biosyst.* **2006**, *2*, 500–508.
- [5] G. Majno, I. Joris, *Am. J. Pathol.* **1995**, *146*, 3–15.
- [6] K. Shiba, *J. Drug Targeting* **2006**, *14*, 512–518.
- [7] M. L. Janmaat, J. A. Rodriguez, J. Jimeno, F. A. E. Kruyt, G. Giaccone, *Mol. Pharmacol.* **2005**, *68*, 502–510.
- [8] D. A. Jeffery, M. Bogoyo, *Curr. Opin. Biotechnol.* **2003**, *14*, 87–95.
- [9] A. M. Piggott, P. Karuso, *Comb. Chem. High Throughput Screening* **2004**, *7*, 607–630; A. M. Piggott, P. Karuso, *Mar. Drugs* **2005**, *3*, 36–63.
- [10] C. M. Crews, J. L. Collins, W. S. Lane, M. L. Snapper, S. L. Schreiber, *J. Biol. Chem.* **1994**, *269*, 15 411–15 414; C. M. Crews, W. S. Lane, S. L. Schreiber, *Proc. Natl. Acad. Sci. USA* **1996**, *93*, 4316–4319.
- [11] K. M. Specht, K. M. Shokat, *Curr. Opin. Cell Biol.* **2002**, *14*, 155–159.
- [12] D. J. Newman, G. M. Cragg, *Chim. Oggi* **2006**, *24*, 42–47.
- [13] S. R. Shengule, P. Karuso, *Org. Lett.* **2006**, *8*, 4083–4084.
- [14] G. P. Smith, V. A. Petrenko, *Chem. Rev.* **1997**, *97*, 391–410.
- [15] P. P. Sche, K. M. McKenzie, J. D. White, D. J. Austin, *Chem. Biol.* **1999**, *6*, 707–716; P. P. Sche, K. M. McKenzie, J. D. White, D. J. Austin, *Chem. Biol.* **2001**, *8*, 399–400.
- [16] K. M. McKenzie, E. J. Vidlock, U. Splittgerber, D. J. Austin, *Angew. Chem.* **2004**, *116*, 4144–4147; *Angew. Chem. Int. Ed.* **2004**, *43*, 4052–4055.
- [17] A. G. Shilabin, N. Kasanah, D. E. Wedge, M. T. Hamann, *J. Med. Chem.* **2007**, *50*, 4340–4350.
- [18] Y. Suárez, L. González, A. Cuadrado, M. Berciano, M. Lafarga, A. Muñoz, *Mol. Cancer Ther.* **2003**, *2*, 863–872.
- [19] S.-I. Fujita, T. Hashimoto, *Int. J. Syst. Evol. Microbiol.* **2000**, *50*, 1381–1389; B. Sancak, J. H. Rex, E. Chen, K. Marr, *J. Clin. Microbiol.* **2004**, *42*, 5889–5891.
- [20] G. Yang, Z. Yang, **2001**.
- [21] J. A. Doudna, V. L. Rath, *Cell* **2002**, *109*, 153–156.
- [22] M. Fromont-Racine, B. Senger, C. Saveanu, F. Fasiolo, *Gene* **2003**, *313*, 17–42.
- [23] M. J. Marion, C. Marion, *FEBS Lett.* **1988**, *232*, 281–285.
- [24] I. G. Wool, *Trends Biochem. Sci.* **1996**, *21*, 164–165; R. A. Zimmermann, *Cell* **2003**, *115*, 130–132; H. Naora, H. Naora, *Immunol. Cell Biol.* **1999**, *77*, 197–205; F. W. Chen, Y. A. Ioannou, *Int. Rev. Immunol.* **1999**, *18*, 429–448; C. D. Lopez, G. Martinovsky, L. Naumovski, *Cancer Lett.* **2002**, *180*, 195–202; N. Khanna, S. Sen, H. Sharma, N. Singh, *Biochem. Biophys. Res. Commun.* **2003**, *304*, 26–35.
- [25] M. Li, M. S. Center, *FEBS Lett.* **1992**, *298*, 142–144.
- [26] T. Adilakshmi, R. O. Laine, *J. Biol. Chem.* **2002**, *277*, 4147–4151.
- [27] S. Volarevic, M. J. Stewart, B. Lederemann, F. Zilberman, L. Terracciano, E. Montini, M. Grompe, S. C. Kozma, G. Thomas, *Science* **2000**, *288*, 2045–2047.
- [28] H. Takashima, *Curr. Top. Med. Chem.* **2003**, *3*, 991–999; S. Magnet, J. S. Blanchard, *Chem. Rev.* **2005**, *105*, 477–497; I. Chopra, M. Roberts, *Microbiol. Mol. Biol. Rev.* **2001**, *65*, 232–260.
- [29] T. Auerbach, A. Bashan, A. Yonath, *Trends Biotechnol.* **2004**, *22*, 570–576; E. Cundliffe, *Biochimie* **1987**, *69*, 863–869.
- [30] H. Teraoka, K. H. Nierhaus, *J. Mol. Biol.* **1978**, *126*, 185–193.
- [31] S. Pestka, *Antimicrob. Agents Chemother.* **1974**, *6*, 474–478.
- [32] A. M. Piggott, P. Karuso, *Tetrahedron Lett.* **2005**, *46*, 8241–8244.
- [33] Novagen (2002). T7Select System Manual TB178 Rev.B 0203. pp. 1–21: USA.

Received: October 11, 2007

Published online on January 25, 2008